JPE 19-5-10

https://doi.org/10.6113/JPE.2019.19.5.1162
ISSN(Print): 1598-2092 / ISSN(Online): 2093-4718

Leg-By-Leg-Based Finite-Control-Set Model Predictive Control for Two-Level Voltage-Source Inverters

Tao Zhang[*,**,***], Xiyou Chen[*], Chen Qi[†], and Zhengying Lang[*]

[†,*]School of Electrical Engineering, Dalian University of Technology, Dalian, China
[**]State Key Lab. of Robotics, Shenyang Institute of Automation, Chinese Academy of Sciences, Shenyang, China
[***]Institutes for Robotics and Intelligent Manufacturing, Chinese Academy of Sciences, Shenyang, China

Abstract

Finite-control-set model predictive control (FCS-MPC) is a promising control scheme for two-level voltage-source inverters (TL-VSIs). However, two main issues arise in the classical FCS-MPC method: an exponentially-increasing computational time and a low steady-state performance. To solve these two issues, a novel FCS-MPC method has been proposed for *n*-phase TL-VSIs in this paper. The basic idea of the proposed method is to carry out the FCS-MPC scheme of TL-VSIs for one leg by one leg, like a "pipeline". Based on this idea, the calculations are reduced from exponential time to linear time and its current waveforms are improved by applying more switching states per sampling period. The cases of three-phase and five-phase TL-VSIs were tested to verify the effectiveness of proposed method.

Key words: Current control, Model predictive control, Two-level voltage-source inverter

I. INTRODUCTION

Two-level voltage-source inverters (TL-VSIs) are used in a wide variety of applications since they can convert a fixed dc voltage into an any-phase ac voltage with a variable magnitude and frequency [1], [2]. The current control of TL-VSIs is one of the most important subjects in power electronics. In the last few decades, several control methods have been proposed [3]-[23]. Some of them, known as indirect controllers, require a modulator to generate the switching signals of a converter, such as proportional-integral (PI) and proportional-resonant (PR) regulators using carrier-based or space vector pulse-width modulation (PWM) techniques [3]. However, when the number of phases is increased, the design difficulty, modulation complexity and implementation costs are also increased in indirect controllers. On the other hand, direct controllers have been introduced with simple concepts and easy digital implementation, where the switching signals are directly determined by reducing the control errors and avoiding the use of modulators [4]-[23]. The hysteresis current control method is the simplest direct controller and it has been extensively used in industry [4].

In the last decade, another direct controller, namely finite-control-set model predictive control (FCS-MPC), has been applied to various power converters [5]-[23], including TL-VSIs [17]-[24]. This method uses the model of a system to predict the future behavior of controlled variables and solves a rolling optimization problem for obtaining desired control actions [5]. By taking advantage of the discrete nature of power converters, the optimization problem is simplified to evaluate all of the switching states and to select the one that minimizes the cost function [6]. The FCS-MPC method has several advantages, including an intuitive concept, fast dynamic response, easy inclusion of system nonlinearities, lack of a modulator, and flexibility to consider various constraints [7]. However, two main issues arise in the classical FCS-MPC method [23], [24].

Manuscript received Jan. 16, 2019; accepted May 18, 2019
Recommended for publication by Associate Editor Yun Zhang.
[†]Corresponding Author: qichen@dlut.edu.cn
Tel: +86-0411-84707894, Dalian University of Technology
[*]School of Electrical Eng., Dalian University of Technology, China
[**]State Key Lab. of Robotics, Shenyang Institute of Automation, Chinese Academy of Sciences, China
[***]Institutes for Robotics and Intelligent Manufacturing, Chinese Academy of Sciences, China

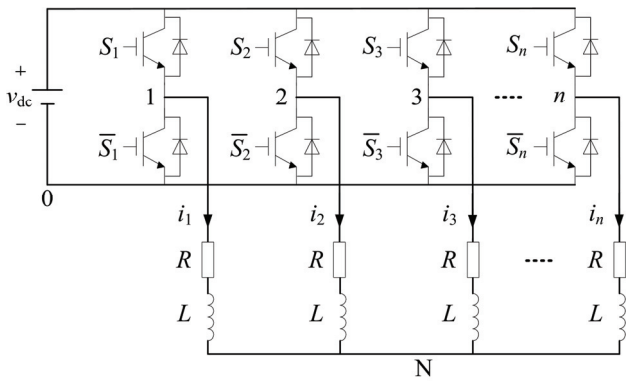

Fig. 1. Topology of a n-phase TL-VSI.

The first is the computational burden associated with the number of switching states. This is especially important for multi-phase TL-VSIs since the number of possible switching states increases exponentially when the number of phases is increased. The second issue is the larger current errors and ripples in steady state because only one switching state is applied for the whole sampling period. Thich, in turn, requires an increased sampling frequency in the classical FCS-MPC method in comparison with modulation-based control methods.

To solve the above-mentioned issues of the classical FCS-MPC method, an improved FCS-MPC method, namely cell-by-cell FCS-MPC, was proposed for single-phase cascaded H-bridge rectifiers in [25], where the FCS-MPC scheme was carried out one cell by one cell, like a "pipeline", leading to a considerable reduction in the computational burden and an improved steady-state performance in comparison with the classical FCS-MPC method. In this paper, this method has been extended to multi-phase TL-VSIs and verified by experiments in the cases of three-phase and five-phase TL-VSIs.

This paper is organized as follows. The prediction model of a TL-VSI is described in Section II. The classical FCS-MPC method is reviewed in Section III, and the proposed method is presented in Section IV. Experimental results are shown in Section V. Finally, the conclusion of this paper is given in Section VI.

II. Prediction Model of a TL-VSI

Fig. 1 shows the topology of an n-phase TL-VSI with a symmetrical passive load, which consists of n half-bridge legs connected in parallel on their dc sides. v_{dc} is the dc voltage. i_i (i=1, 2, …, n) is the output current of the ith leg. S_i and $\overline{S}_i$ stand for the upper and lower switches of the ith leg, and they are complementary.

It is known that to completely describe an n-phase system, representations of the system variables in multiple α-β stationary reference frames (planes) must be adopted [26]. With the concept of decomposition, the n-phase variables are mapped into the α_1-β_1 and α_h-β_h (h=3, 5, …, n-2) planes as:

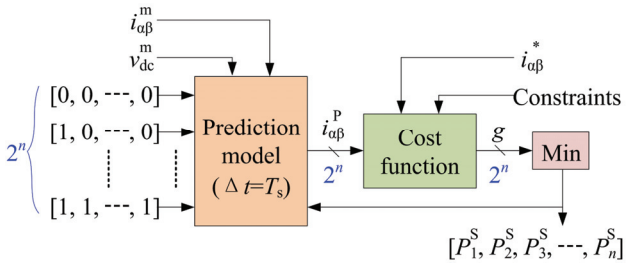

Fig. 2. Block diagram of the classical FCS-MPC method.

$$\mathbf{x}_{\alpha\beta} = \mathbf{T}\mathbf{x} \tag{1}$$

where $\mathbf{x}=[x_1, x_2, \ldots, x_n]^T$ represents the vector of certain variables of the system in terms of phase values, while $\mathbf{x}_{\alpha\beta}=[x_{\alpha1}, x_{\beta1}, x_{\alpha3}, x_{\beta3}, \ldots, x_{\alpha h}, x_{\beta h}]^T$ represents the vector of the variables in the transformed plane. $\mathbf{T}$ is the decomposition transformation matrix. For an n-phase system with an equally distributed phase angle θ (=360°/n), $\mathbf{T}$ is given as:

$$\mathbf{T}=\frac{2}{n}\begin{bmatrix} 1 & \cos\theta & \cos 2\theta & \cdots & \cos(n-1)\theta \\ 0 & \sin\theta & \sin 2\theta & \cdots & \sin(n-1)\theta \\ 1 & \cos 3\theta & \cos 6\theta & \cdots & \cos 3(n-1)\theta \\ 0 & \sin 3\theta & \sin 6\theta & \cdots & \sin 3(n-1)\theta \\ \vdots & \vdots & \vdots & \vdots & \vdots \\ 1 & \cos(n-2)\theta & \cos 2(n-2)\theta & \cdots & \cos(n-1)(n-2)\theta \\ 0 & \sin(n-2)\theta & \sin 2(n-2)\theta & \cdots & \sin(n-1)(n-2)\theta \end{bmatrix} \tag{2}$$

The output current of an n-phase TL-VSI with an RL load can be calculated in the transformed plane as:

$$\mathbf{i}_{\alpha\beta}(t+\Delta t)=(1-\frac{R}{L}\Delta t)\mathbf{i}_{\alpha\beta}(t)+\frac{\Delta t}{L}\mathbf{v}_{\alpha\beta}(t) \tag{3}$$

where Δt is a prediction time interval and:

$$\mathbf{i}_{\alpha\beta}(t)=\mathbf{T}\mathbf{i}^T=\mathbf{T}\begin{bmatrix} i_1(t) & i_2(t) & \cdots & i_n(t)\end{bmatrix}^T \tag{4a}$$

$$\mathbf{v}_{\alpha\beta}(t)=\mathbf{T}\mathbf{v}_N^T=\mathbf{T}\begin{bmatrix} v_{1N}(t) & v_{2N}(t) & \cdots & v_{nN}(t)\end{bmatrix}^T \tag{4b}$$

In (4b), v_{iN} is the output phase voltage of the ith leg, and can be calculated as:

$$v_{iN}=\frac{1}{n}(nv_{i0}-\sum_{k=1}^{n}v_{k0}) \tag{5}$$

where v_{i0} is the ith leg voltage, and can be calculated as:

$$v_{i0}=P_i v_{dc} \tag{6}$$

where P_i is the switching function of the ith leg. P_i is 1 when S_i is turned on. Otherwise, P_i is 0.

III. Classical FCS-MPC Method

The classical FCS-MPC method is described in this section for comparison. Fig. 2 shows a block diagram of the classical FCS-MPC method for an n-phase TL-VSI, where the superscripts m, P, S, and * mean the measured, predicted, selected, and reference variables, respectively. Here, Δt is

TABLE I
TOTAL NUMBER OF CONSIDERED SWITCHING FUNCTION VECTORS

No. of phases	No. of considered switch function vectors	
	Classical method	Proposed method
5	32	10
6	64	12
7	128	14
n	2^n	$2n$

equal to the sampling period T_s. The classical FCS-MPC is a complete-enumeration-based predictive control method. As shown in Fig. 2, the optimal switching function vector $[P_1^s, P_2^s, P_3^s, \cdots, P_n^s]$ is selected by evaluating the cost function for all of the possible switching function vectors.

To achieve current tracking for an n-phase TL-VSI, the cost function can be defined as:

$$g = \sum_{j=1}^{n-2}(i_{\alpha j}^* - i_{\alpha j})^2 + \sum_{j=1}^{n-2}(i_{\beta j}^* - i_{\beta j})^2 \quad (7)$$

To compensate the calculation delay caused by the update mechanism in digital controllers, two-step-forward prediction is required in the FCS-MPC method [5].

Considering the two available values 0 and 1 of the switching function P_i for each leg, there are 2^n switching function vectors in total for an n-phase TL-VSI. In the classical FCS-MPC method, the computational burden increases exponentially when the number of phases is increased, as shown in Table I. Consequently, it is difficult to implement the control algorithm using a standard digital controller, especially when a high sampling frequency is required.

IV. PROPOSED METHOD

To reduce the computational burden without losing the intuitive and general concept of the classical FCS-MPC method, a novel FCS-MPC method for an n-phase TL-VSI has been proposed in this paper. Fig. 3 shows a block diagram of the proposed method, which is composed of n identical control blocks for n legs. The optimal switching function P_i^S of each leg is selected sequentially from the first control block to the last control block. Like the classical FCS-MPC method shown in Fig. 2, each control block of the proposed method shown in Fig. 3 is an enumeration-based predictive control technique. Thus, the proposed method inherits the intuitive and general concept of the classical FCS-MPC method.

To make the proposed method easy to understand, the basic idea of how to carry out the FCS-MPC scheme for one leg by one leg is shown in Fig. 4. It can be noted in Fig. 4 that the sampling period Ts is divided the into n equal intervals for an n-phase TL-VSI. In each interval, only one leg can change its switching state while the other legs have the same switching states as those applied in the last interval. The change instant of the switching state is fixed at the beginning

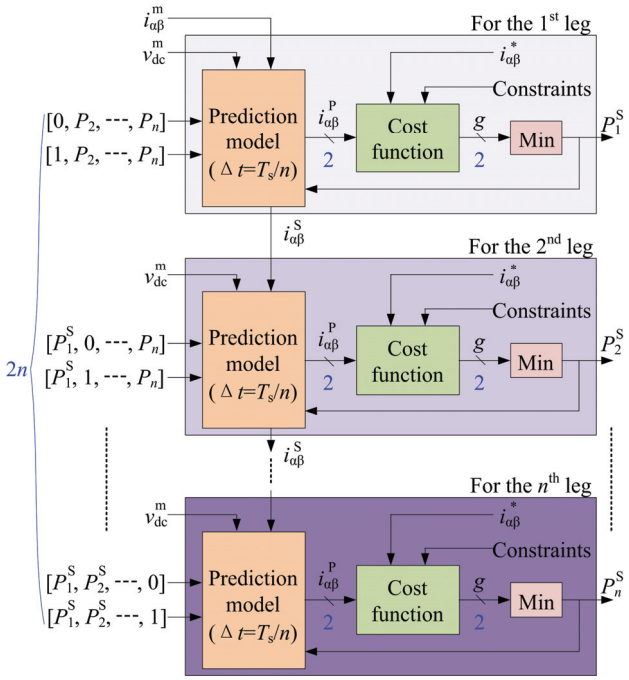

Fig. 3. Block diagram of the proposed method.

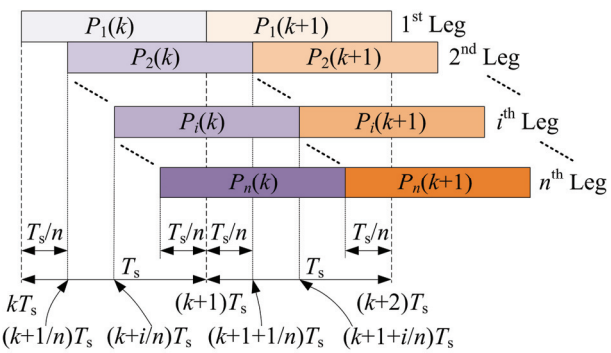

Fig. 4. Basic idea of the proposed method.

of the interval and the optimal switching state of each leg is applied for one whole sampling period. For example, $P_2(k)$ starts from the instant $(k+1/n)T_s$ and ends at the instant $(k+1+1/n)T_s$. From the first interval to the last interval, the prediction of the controlled variables is completed sequentially and the optimal switching function P_i^S of the leg is selected one by one. For the prediction of the next leg, as shown in Fig. 3, the output current $i_{\alpha\beta}^S$ at the end of the current interval is required and it can be calculated on the basis of the current available at the beginning of the current interval and the selected switching function of the current leg.

Only two possible switching function vectors are considered for each leg. Consequently, the total number of considered switching function vectors in the proposed method is the twice number of phases. In other words, an increased number of legs increases the calculation time linearly, as shown in Table I. A considerable reduction of the computational burden can be achieved in the proposed method in comparison with the

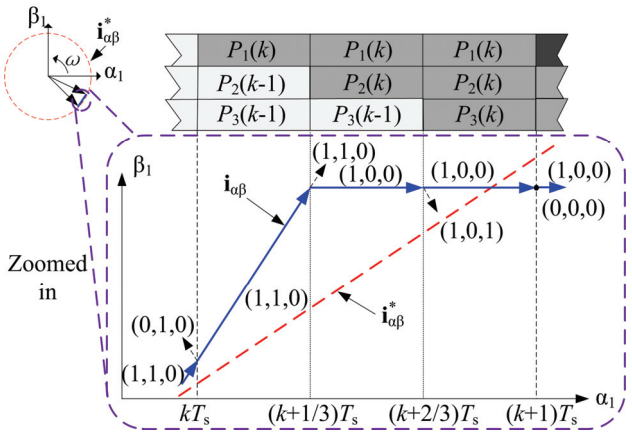

Fig. 5. Illustrations of current vector trajectories generated by the proposed method in the α_1-β_1 plane.

classical FCS-MPC method. For example, when n is 7, the number of considered switching function vectors is 14 in the proposed method. However, it is 128 in the classical FCS-MPC method. Because of its low complexity and simple scheme, the proposed method can be easily extended to a TL-VSI with any number of phases.

Unlike the classical FCS-MPC method, which selects only one switching states to be applied for a whole sampling period, the proposed method can generate multiple switching states per sampling period, which provides a chance to reduce current errors and ripples without increasing the sampling frequency, as shown in Fig. 5, where the current trajectories in the α_1-β_1 plane are illustrated.

The calculation flow of the proposed method is as follows.

(1) Measure i_1, i_2, i_3, …, i_n at the instant kT_s.

(2) Calculate $i_{\alpha 1}$, $i_{\beta 1}$, …, $i_{\alpha h}$, $i_{\beta h}$ at the instant $(k+1)T_s$ for delay compensation.

(3) Predict $i_{\alpha 1}$, $i_{\beta 1}$, …, $i_{\alpha h}$, $i_{\beta h}$ at the end $(k+1+i/n)T_s$ of the ith interval of the next sampling period for the ith leg.

(4) Calculate the cost function g given in (7) for two candidates of the ith leg.

(5) Select the optimal switching function P_i^s of the ith leg by minimizing g.

(6) Repeat steps (3)-(5) for the other legs one by one.

V. Experimental Results

An experimental platform of a five-phase TL-VSI with a RL load was built in the laboratory and shown in Fig. 6. The proposed method along with the classical FCS-MPC method are implemented on a TMS320F28335 digital signal processor (DSP). The constant dc voltage is generated by using a diode bridge and dc capacitors. The experimental parameters are listed in Table II, where T_d is the dead time of the gate signals. To verify the effectiveness of the proposed method, the experimental tests through case studies have been carried out. The examined cases are three-phase and five-phase TL-VSIs.

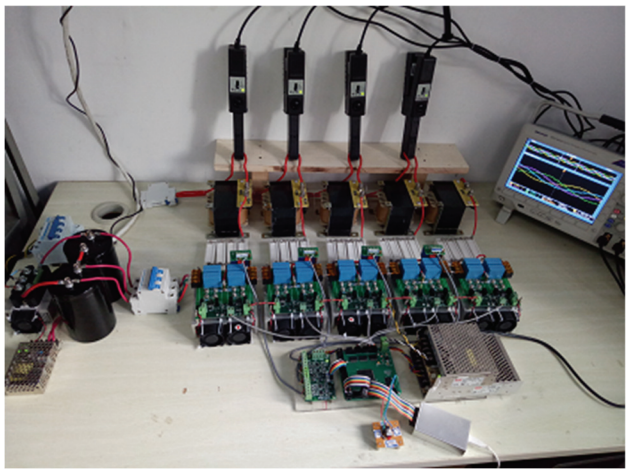

Fig. 6. Experimental platform.

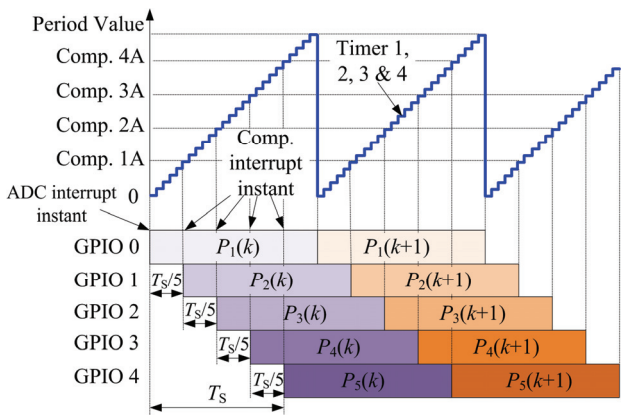

Fig. 7. Digital implementation scheme based on a timer interrupt.

TABLE II
Experimental Parameters

v_{dc}	30V	T_d	2us	R/L	2.5Ω/10mH

Fig. 7 shows the digital implementation scheme based on the timer interrupt on the DSP. On the TMS320F28335 DSP, six EPWM modules are available and each of them provides one timer and two comparators A and B. An interrupt can occur in each EPWM module when the timer value is equal to the comparator value. The switching signals generated by the GPIO on the DSP can be controlled by an interrupt event. Taking the five-phase TL-VSI as an example, as shown in Fig. 7, the switching function $P_2(k)$ for the second leg is achieved at the comparator 1A interrupt instant. This instant can be controlled by calculating the comparator value. One more interrupt is necessary to achieve the output voltage transition at the beginning of a sampling period. The ADC module on the DSP can provide this interrupt event which occurs when the timer value returns to zero.

A. Computational Time

Table III shows the computation times needed for the classical FCS-MPC method and the proposed method, which

TABLE III
COMPUTATION TIME

Control method	Computational time	
	Three-phase	Five-phase
Classical method	7.322μs	36.55μs
Proposed method	5.838μs	16.8μs

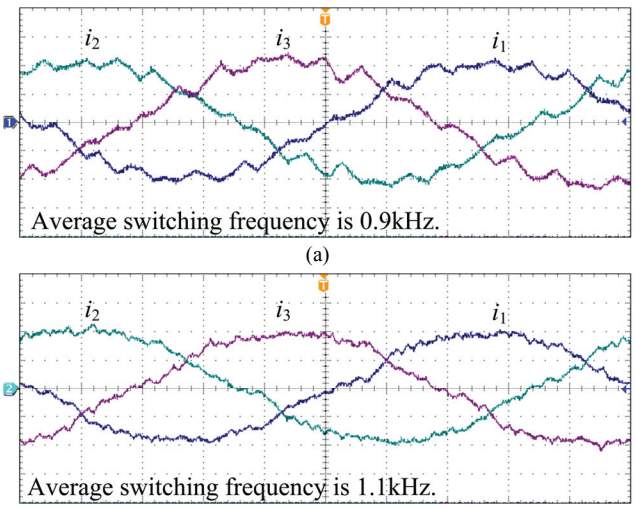

Fig. 8. Steady-state waveforms of the output currents of a three-phase TL-VSI for: (a) Classical FCS-MPC method; (b) Proposed method at the same sampling frequency f_s=5kHz (Current: 1A/div; Time: 2ms/div).

are measured by generating a pulse whose width equal to the execution time of the program in the DSP controller. As shown in Table III, the proposed method has a significant reduction in computational time in comparison with the classical FCS-MPC method.

B. Steady-State Performance

Fig. 8 and Fig. 9 show steady-state experimental waveforms of the output currents of three-phase and five-phase TL-VSIs for the classical FCS-MPC method and the proposed method when the sampling frequency f_s is 5kHz. The sinusoidal reference output current of each leg with an amplitude of 2A and a frequency of 50Hz is generated in the DSP program. More evaluations are shown in Fig. 10, where the THD of the output current and average switching frequency f_{sw} at different sampling frequencies for the classical FCS-MPC method and the proposed method are given.

The average switching frequency can be computed in the DSP with a moving average window of M data-elements as:

$$f_{sw}=\frac{1}{nMT_s}\sum_{i=1}^{n}\sum_{l=1}^{M}n_{ci}(k+1-l) \tag{8}$$

where n_{ci} is the number of switchings in the ith leg per sampling period. n_{ci} is equal to 1 when commutation occurs on this leg. M is set as 1000, which is large enough to obtain a fixed average switching frequency.

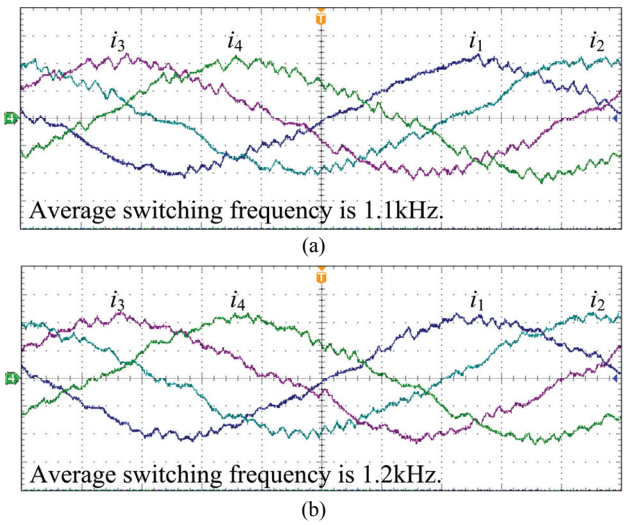

Fig. 9. Steady-state waveforms of the output currents of a five-phase TL-VSI for: (a) Classical FCS-MPC method; (b) Proposed method at the same sampling frequency f_s=5kHz (Current: 1A/div; Time: 2ms/div).

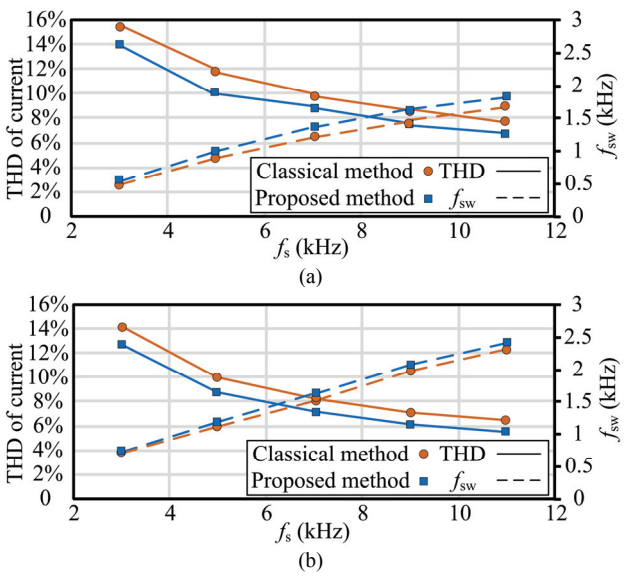

Fig. 10. Comparisons of the THD of the current and the average switching frequency for the classical FCS-MPC method and the proposed method for TL-VSIs at different sampling frequencies. (a) Three-phase. (b) Five-phase.

It can be noted in Fig. 10 that an increase in the sampling frequency leads to a reduction in the THD of the current but an increase in the average switching frequency for both methods. When the sampling frequency stays the same, the THD of the output currents is smaller in the proposed method than that in the classical FCS-MPC method at the expense of an increased average switching frequency.

By carrying out the FCS-MPC scheme for one leg by one leg, the proposed method may generate more switching states per sampling period and have a higher switching frequency than the classical FCS-MPC method. According to (8), the maximum average switching frequency of the proposed method

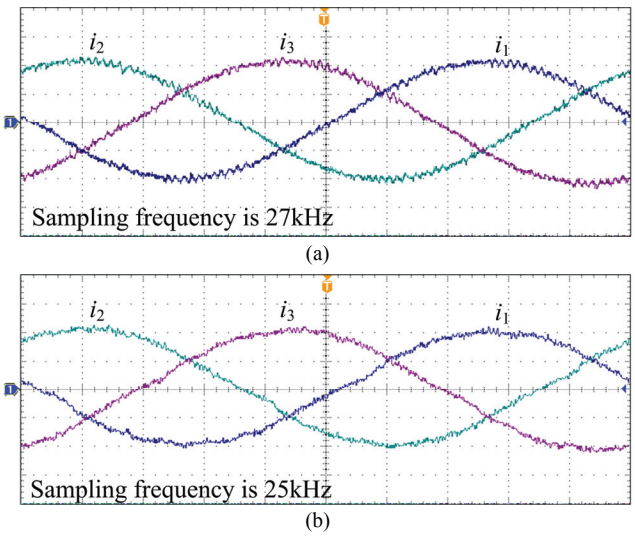

Fig. 11. Steady-state waveforms of the output currents of a three-phase TL-VSI for: (a) Classical FCS-MPC method; (b) Proposed method at the same average switching frequency f_{sw}=5kHz (Current: 1A/div; Time: 2ms/div).

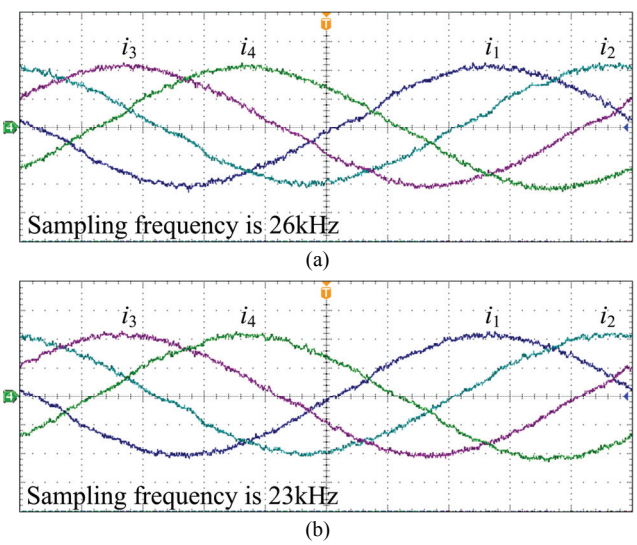

Fig. 12. Steady-state waveforms of the output currents of a five-phase TL-VSI for: (a) Classical FCS-MPC method; (b) Proposed method at same average switching frequency f_{sw}=5kHz (Current: 1A/div; Time: 2ms/div).

is equal to the sampling frequency only if each leg changes its switching state per sampling period. In practice, since only small parts of the legs have switchings per sampling period, the average switching frequency of the proposed method is much lower than the sampling frequency. However, it is slightly higher than the classical FCS-MPC method.

The average switching frequency is proportional to the sampling frequency. More comparisons are shown in Fig. 11 and Fig. 12, where the same average switching frequency f_{sw} of 5kHz for both methods can be achieved by carefully tuning the sampling frequency. Because of a big increase in the sampling frequency, the THDs of the currents in Fig. 11 and

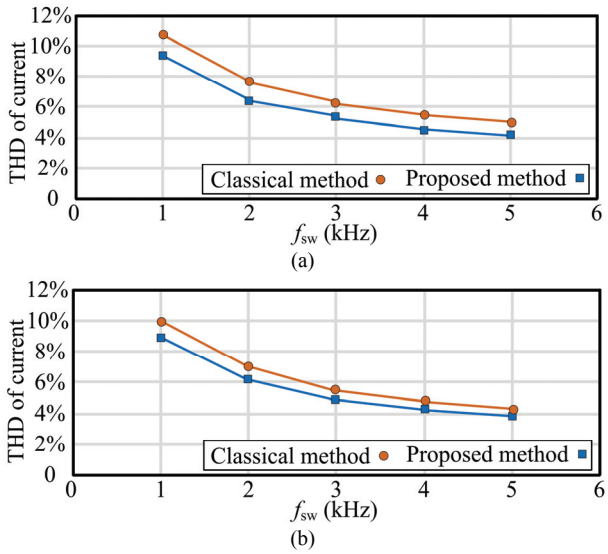

Fig. 13. Comparisons of THD of current for classical FCS-MPC method and proposed method of: (a) Three-phase; (b) Five-phase TL-VSIs at different average switching frequencies.

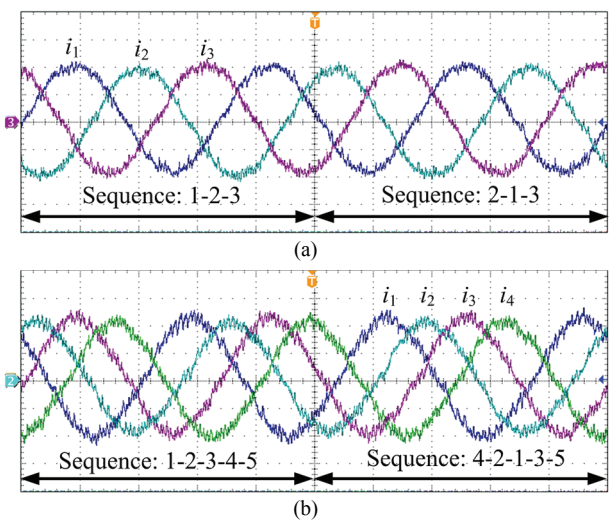

Fig. 14. Current waveforms of the proposed method for TL-VSIs under different prediction sequences: (a) Three-phase; (b) Five-phase (Current: 1A/div; Time: 10ms/div).

Fig. 12 are much lower than those in Fig. 8 and Fig. 9. However, as shown in Table III, it is hard to make a further increase in the sampling frequency for the classical FCS-MPC method since it will exceed the limitation on computational time. On the other hand, a much larger margin to increase the sampling frequency is available in the proposed method, which can lead to a further enhancement of the steady-state control performance.

Fig. 13 shows the THD of output current at different average switching frequencies for the classical FCS-MPC method and the proposed method. It can be noted in Fig. 13 that the proposed method has a smaller THD of the current than the classical FCS-MPC method even under the same average switching frequency.

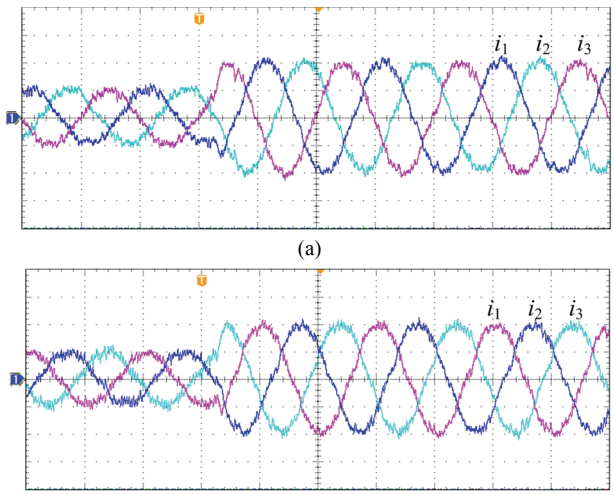

Fig. 15. Dynamic responses of the output currents of a three-phase TL-VSI for: (a) Classical FCS-MPC method; (b) Proposed method with a step change of the reference currents from 1A to 2A (Current: 1A/div; Time: 10ms/div).

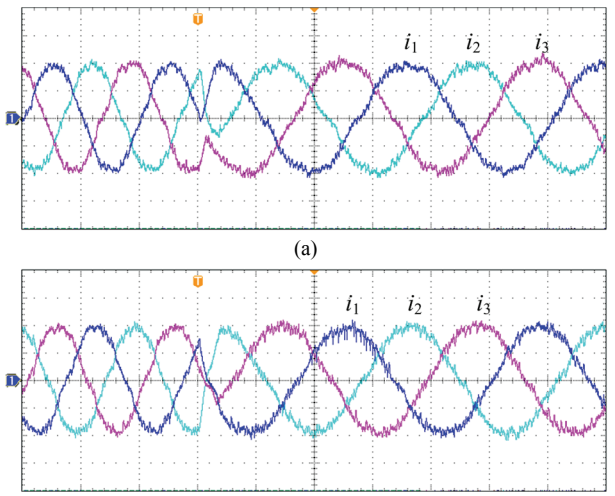

Fig. 17. Dynamic responses of the output currents of a three-phase TL-VSI for: (a) Classical FCS-MPC method; (b) Proposed method with a step change of the reference currents from 50Hz to 30Hz (Current: 1A/div; Time: 10ms/div).

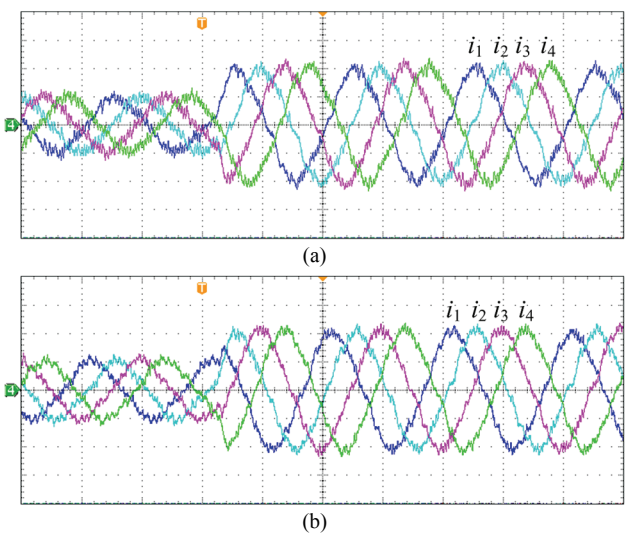

Fig. 16. Dynamic responses of the output currents of a five-phase TL-VSI for: (a) Classical FCS-MPC method; (b) Proposed method with a step change of the reference currents from 1A to 2A (Current: 1A/div; Time: 10ms/div).

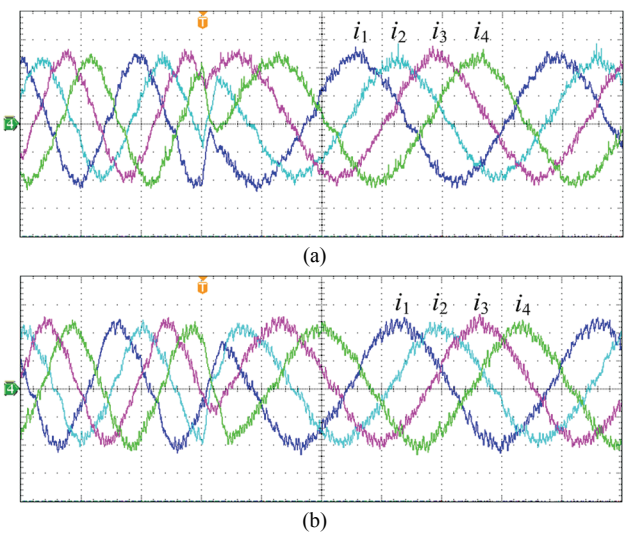

Fig. 18. Dynamic responses of the output currents of a five-phase TL-VSI for: (a) Classical FCS-MPC method; (b) Proposed method with a step change of the reference currents from 50Hz to 30Hz (Current: 1A/div; Time: 10ms/div).

The output switching states are dependent on the prediction sequence for the legs. Nevertheless, current waveforms are rarely affected under different prediction sequences, as illustrated in Fig. 14.

C. Dynamic Performance

The dynamic performances of the classical FCS-MPC method and the proposed method are shown in Fig. 15-18, where the step changes of the reference currents from 1A to 2A and from 50Hz to 30Hz are evaluated. It can be seen in Fig. 15-18 that the proposed method has a comparable dynamic performance in comparison with the classical FCS-MPC method. Although the proposed method does not allow for a simultaneous change in all of the leg voltages, a small reduction in the dynamic response is barely noticeable due to the inertia of the load.

VI. CONCLUSIONS

This paper proposed a novel FCS-MPC method for TL-VSIs. By carrying out a FCS-MPC scheme for one leg by one leg, the proposed method has an enhanced steady-state current performance along with a reduced computational burden without sacrificing dynamic performance when compared with the classical FCS-MPC method. The proposed method inherits the intuitiveness and general concept of the classical

FCS-MPC method. Thus, the proposed method can be easily extended to a TL-VSI with any number of phases. Finally, experimental comparisons between proposed method and the classical FCS-MPC method have been made through case studies of three-phase and five-phase TL-VSIs. The experimental results show that a reduced computational time and an enhanced current control performance are achieved in the proposed method.

ACKNOWLEDGMENT

This work was supported in part by the National Science and Technology Major Project (2017ZX02101007-004), in part by the PhD Staring Foundation of Liaoning Province of China (20170520112), and in part by the Fundamental Research Funds for the Central Universities (DUT19JC07 and DUT1 9RC(4)019).

REFERENCES

[1] J. I. Leon, S. Kouro, L. G. Franquelo, J. Rodriguez, and B. Wu, "The essential role and the continuous evolution of modulation techniques for voltage-source inverters in the past, present, and future power electronics," *IEEE Trans. Ind. Electron*., Vol. 63, No. 5, pp. 2688-2701, May 2016.

[2] D. Casadei, D. Dujic, E. Levi, G. Serra, A. Tani, and L. Zarri, "General modulation strategy for seven-phase inverters with independent control of multiple voltage space vectors," *IEEE Trans. Ind. Electron*., Vol. 55, No. 5, pp. 1921-1932, May 2008.

[3] D. G. Holmes and T. A. Lipo, Pulse Width Modulation for Power Converters: Principles and Practice, IEEE Press, 2003.

[4] N. Mohan, T. M. Undeland, and W. P. Robbins, *Power Electronics – Converters, Applications and Design*, 3rd ed., Media Enhanced Edition, Wiley, 2003.

[5] S. Kouro, P. Cortes, R. Vargas, U. Ammann, and J. Rodriguez, "Model predictive control – A simple and powerful method to control power converters," *IEEE Trans. Ind. Electron*., Vol. 56, No. 6, pp. 1826-1838, Jun. 2009.

[6] J. Holtz, "Advanced pwm and predictive control—an overview," *IEEE Trans. Ind. Electron*., Vol. 63, No. 6, pp. 3837-3844, Jun. 2016.

[7] S. Vazquez, J. Rodriguez, M. Rivera, L. G. Franquelo, and M. Norambuena, "Model predictive control for power converters and drives: advances and trends," *IEEE Trans. Ind. Electron*., Vol. 64, No. 2, pp. 935-947, Feb. 2017.

[8] C. Xia, T. Liu, T. Shi, and Z. Song, "A simplified finite-control-set model-predictive control for power converters," *IEEE Trans. Ind. Informat.*, Vol. 10, No. 2, pp. 991-1002, May. 2014.

[9] W. Xie, X. Wang, F. Wang, W. Xu, R. M. Kennel, D. Gerling, and R. D. Lorenz, "Finite-control-set model predictive torque control with a deadbeat solution for PMSM Drives," *IEEE Trans. Ind. Electron*., Vol. 62, No. 9, pp. 5402-5410, Sep. 2015.

[10] Z. Zhang, C. M. Hackl, and R. Kennel, "Computationally Efficient DMPC for three-level NPC back-to-back convertersin wind turbine systems with PMSG," *IEEE Trans. Power Electron*., Vol. 32, No. 10, pp. 8018-8034, Oct. 2017.

[11] X. Wang and D. Sun, "Three-vector based low-complexity model predictive direct power control strategy for doubly fed induction generator," *IEEE Trans. Power Electron*., Vol. 32, No. 1, pp. 773-782, Jan. 2017.

[12] W. Song, J. Ma, L. Zhou, and X. Feng, "Deadbeat predictive power control of single-phase three-level neutral-point-clamped converters using space-vector modulation for electric railway traction," *IEEE Trans. Power Electron*., Vol. 31, No. 1, pp. 721-732, Jan. 2016.

[13] C. Cheng, H. Nian, X. Wang, and D. Sun, "Deadbeat predictive direct power control of voltage source inverters with optimised switching patterns," *IET Power Electron*., Vol. 10, No. 12, pp. 1438-1451, Dec. 2017.

[14] C. Qi, X. Chen, P. Tu, and P. Wang, "Deadbeat control for a single-phase cascaded H-bridge rectifier with voltage balancing modulation," *IET Power Electron*., Vol. 11, No. 3, pp. 610-617, Mar. 2018.

[15] A. Dekka, B. Wu, V. Yaramasu, and N. R. Zargari, "Dual-stage model predictive control with improved harmonic performance for modular multilevel converter," *IEEE Trans. Ind. Electron*., Vol. 63, No. 10, pp. 6010-6019, Oct. 2016.

[16] T. Geyer, "Computationally efficient model predictive direct torque control," *IEEE Trans. Power Electron*., Vol. 26, No. 10, pp. 2804-2816, Oct. 2011.

[17] F. Barrero, M. R. Arahal, R. Gregor, S. Toral, and M. J. Duran, "A proof of concept study of predictive current control for vsi-driven asymmetrical dual three-phase ac machines," *IEEE Trans. Ind. Electron*., Vol. 56, No. 6, pp. 1937-1954, Jun. 2009.

[18] F. Barrero, M. R. Arahal, R. Gregor, S. Toral, and M. J. Duran, "One-step modulation predictive current control method for the asymmetrical dual three-phase induction machine," *IEEE Trans. Ind. Electron*., Vol. 56, No. 6, pp. 1974-1983, Jun. 2009.

[19] M. J. Duran, J. Prieto, F. Barrero, and S. Toral, "Predictive current control of dual three-phase drives using restrained search techniques," *IEEE Trans. Ind. Electron*., Vol. 58, No. 8, pp. 3253-3263, Aug. 2011.

[20] F. Barrero, J. Prieto, E. Levi, R. Gregor, S. Toral, M. J. Duran, and M. Jones, "An enhanced predictive current control method for asymmetrical six-phase motor drives," *IEEE Trans. Ind. Electron*., Vol. 58, No. 8, pp. 3242-3252, Aug. 2011.

[21] M. J. Duran, J. A. Riveros, F. Barrero, H. Guzman, and J. Prieto, "Reduction of common-mode voltage in five-phase induction motor drives using predictive control techniques," *IEEE Trans. Ind. Applicat*., Vol. 48, No. 6, pp.2059-2067, Nov./Dec. 2012.

[22] J. A. Riveros, F. Barrero, E. Levi, M. J. Duran, S. Toral, and M. Jones, "Variable-speed five-phase induction motor drive based on predictive torque control," *IEEE Trans. Ind. Electron*., Vol. 60, No. 8, pp. 2957-2968, Aug. 2013.

[23] C. S. Lim, E. Levi, M. Jones, N. A. Rahim, and W. P. Hew, "FCS-MPC-based current control of a five-phase induction motor and its comparison with pi-pwm control," *IEEE Trans. Ind. Electron*., Vol. 61, No. 1, pp. 149-163, Jan. 2014.

[24] M. Cheng, F. Yu, K. T. Chau, and W. Hua, "Dynamic performance evaluation of a nine-phase flux-switching permanent-magnet motor drive with model predictive control," *IEEE Trans. Ind. Electron*., Vol. 63, No. 7, pp. 4539-4549, Jul. 2016.

[25] C. Qi, X. Chen, P. Tu, and P. Wang, "Cell-by-cell-based finite-control-set model predictive control for a single-phase cascaded h-bridge rectifier," *IEEE Trans. Power Electron*., Vol. 33, No. 2, pp. 1654 - 1665, Feb. 2018.

[26] Y. Zhao and T. A. Lipo, "Space vector PWM control of dual three-phase induction machine using vector space decomposition," *IEEE Trans. Ind. Appl*., Vol. 31, No. 5, pp.1100-1109, Sep./Oct. 1995.

Tao Zhang received his B.S. and M.S. degrees in Electrical Engineering from the Dalian University of Technology, Dalian, China, in 2009 and 2011, respectively. He is presently a part-time Ph.D. student at the Dalian University of Technology. Since 2012, he has been with the State Key Laboratory of Robotics, Shenyang Institute of Automation, Chinese Academy of Sciences, Shenyang, China, where he is presently working as an Assistant Researcher. His current research interests include model predictive control, servo drives, high power linear amplifiers, and drive-control integrated systems.

Xiyou Chen received his B.S., M.S. and Ph.D. degrees in Electrical Engineering from the Harbin Institute of Technology, Harbin, China, in 1982, 1985 and 2000, respectively. From April 2004 to March 2005, he was a Visiting Scholar in the Department of Electrical and Computer Engineering, University of Waterloo, Waterloo, ON, Canada. He is presently working as a Professor in the School of Electrical Engineering, Dalian University of Technology, Dalian, China. His current research interests include matrix converters and wireless power transfer.

Chen Qi received his B.S. and Ph.D. degrees in Electrical Engineering from the School of Electrical Engineering, Dalian University of Technology, Dalian, China, in 2009 and 2014, respectively. From April 2015 to October 2016, he worked as a Postdoctoral Fellow in the Rolls-Royce @ NTU Corporate Lab, Nanyang Technological University, Singapore. Since November 2016, he has been with the Dalian University of Technology, Dalian, China, where his is presently working as an Assistant Professor. His current research interests include multilevel converters, matrix converters, model predictive control, random modulation, and wireless power transfer.

Zhengying Lang received her B.S. degree in Electrical Engineering from the Dalian University of Technology, Dalian, China, in 2018, where he is presently working toward her M.S. degree in Electrical Engineering. Her current research interests include wireless power transfer.